

Hunting for extra dimensions in black hole shadows

A. S. Lemos^{1,2,*} J. A. V. Campos^{2,†} and F. A. Brito^{2,3,‡}

¹*Departamento de Ciências Exatas e Tecnologia da Informação,
Universidade Federal Rural do Semi-Árido,
59515-000 Angicos, Rio Grande do Norte, Brazil*

²*Departamento de Física, Universidade Federal de Campina Grande,
Caixa Postal 10071, 58429-900 Campina Grande, Paraíba, Brazil*

³*Departamento de Física, Universidade Federal da Paraíba,
Caixa Postal 5008, 58051-970 João Pessoa, Paraíba, Brazil*

Abstract

Observational data of the Sagittarius A* (Sgr A*) shadow released by the Event Horizon Telescope (EHT) are used to investigate eventual deviations in the black hole shadow radius, aiming to seek physics beyond the Standard Model (SM) coming from extra-dimensional theory. We consider the brane-world scenario described by the Randall-Sundrum model and determine the black hole shadow radius correction owing to the higher dimension. From data of the shadow radius in units of BH mass determined by KECK- and VLTI-based estimates, we imposed restrictions on the deviation obtained, and one sets an upper limit to the curvature radius of Anti-de Sitter (AdS_5) spacetime $\ell \lesssim 4.3 \times 10^{-2}$ AU (at 95% confidence level).

*Electronic address: adiel@ufersa.edu.br

†Electronic address: joseandrecampos@gmail.com

‡Electronic address: fabrito@df.ufcg.edu.br

I. INTRODUCTION

Over the last century, attempts have been made to investigate the geometrical structure of the Universe from the proposal of the existence of extra dimensions [1]. Following the development of general relativity, a theoretical extra-dimensional model was built, which aimed to unify the electromagnetic and gravitational fields [2, 3]. Recently, the modern brane-world theories have renewed interest in higher dimensional theories [4–8]. These proposed models arise in the unification schemes, where one expected that the unification of gravitational and gauge forces would occur near the TeV scale [4–6]. In such case, the gauge interactions, and therefore the ordinary matter, get confined to a 4-dimensional hypersurface (3-brane), whereas gravity lives in a higher-dimensional spacetime known as bulk [7, 8]. Thus, gravity would be diluted in the higher-dimensional space, spreading throughout the bulk, explaining, therefore, the observed weakness of gravity compared to other fundamental interactions of nature [4–8]. Consequently, this is a promising scenario to address the hierarchy problem that deals with the discrepancy between the gravitational and electroweak fundamental energy scales without relying on low-energy supersymmetry or technicolor [4–6].

In this framework, although the Standard Model (SM) fields are trapped on our 4-dimensional manifold, events of high-energy collisions can, for instance, eventually cause the SM particles to be kicked off into the new dimensions [9]. Thus, collider experiments have been employed to seek for evidence of large extra dimensions in Arkani-Hamed-Dimopoulos-Dvali (ADD) model, and it was found that the most stringent limits on the Planck mass of higher-dimensional spacetime come from ATLAS (CMS) missing energy experiment, giving $M_D > 5.9 - 11.2$ TeV [10]. In its turn, analysis from astrophysical and cosmological origin, such as light KK gravitons production in stars, has also provided the strongest bounds so that $M_D > 1700 (76)$ TeV for $\delta = 2 (3)$ [11]. Further discussions have attempted to seek traces of extra dimensions in several physical systems, such as in rotating torsion balance [12, 13] – wherein one tests Newton’s law at sub-mm distances –, spectroscopy and atomic physics [14–21], and black hole production [22, 23].

On the other hand, the model proposed by Randall and Sundrum (RS) [7, 8] describes our universe by postulating it as a five-dimensional Anti-de Sitter (AdS_5) spacetime with a warped geometry. In this scenario, bounds on the AdS_5 curvature radius ℓ have also been imposed from astrophysical observations. For instance, the investigation of the persistence

of X-ray binaries containing a black hole in an AdS_5 brane-world shows that $\ell \lesssim 10^{-2} \text{ mm}$ [24]. Furthermore, recent work has also aimed to search for signals of the extra dimension on events of black hole gravitational waves [25, 26]. In such a way, the study of Hawking radiation emitted by stellar-mass black holes found that $\ell \lesssim 5 \mu\text{m}$ from gravitational wave measurements [27], while Ref. [28] – analyzing the shadow of M87* – imposes constraints on the AdS_5 radius such that $\ell \lesssim 170 \text{ AU}$. The multi-messenger cosmology, which considers joint observations of gravitational waves and electromagnetic counterparts, has been used to set limits on the radius of curvature of the higher-dimensional spacetime, $\ell \lesssim 0.535 \text{ Mpc}$ [29]. On its turn, Ref. [30] constrains the tidal charge of a rotating brane-world black hole.

It is known that the black holes only recently have been experimentally probed. Such observations may provide us with significant insights into the structure of spacetime. In this context, the LIGO-VIRGO collaboration has been responsible for presenting empirical data on gravitational wave events from the merger of binary black hole system and neutron stars [31, 32]. In the black hole merger process a ringdown phase arises from the gravitational wave signal, and in this scenario the study of quasinormal modes (QNMs) has been attracting interest in recent years [33–37]. Quasinormal modes are solutions of perturbation equations that have complex characteristic oscillation frequencies that satisfy specific boundary conditions [38]. The QNMs can be obtained using approximative methods, such as Wentzel-Kramers-Brillouin (WKB) approximation or other numerical methods, in different orders of precision [39–42].

In higher-dimensional theories, QNMs have gained increasing attention in recent years [41, 43–47], once one expects such investigations may reveal signals of extra dimensions. In turn, recent measurements of the Event Horizon Telescope (EHT) provided images of supermassive black hole shadow at the M87* galaxy center [48, 49], in addition to the shadow of compact source Sagittarius A* (Sgr A*), a supermassive black hole in the center of the Milky Way [50, 51]. It is noteworthy that, in this scenario, the search for physics beyond the SM has been based on analysis of the shadow radius and deviation from the circularity ΔC of the shadow. However, whereas the circularity has been quoted for the M87* measurements, such information for Sgr A* observational data is not available. Therefore, the approach employed in Ref. [28] cannot be applied to test fundamental physics from the circularity deviations of Sgr A*, and one must recover to investigations based on its shadow size. In the present work, we aim to determine conservative constraints on the AdS_5 radius of curvature

from observational data of the shadow of Sgr A*. For this purpose, we will consider a black hole in the RS background in the weak field regime, described by the Garriga-Tanaka metric [52]. This solution has been obtained by assuming a classic approach that provides the linearized brane-world gravity. As we will see, our analysis allowed us to place the bounds on the extra-dimensional curvature radius ℓ in an alternative way, avoiding the issue of lack of circularity measures for Sgr A* and exploring its inaccurate spin measurements [53, 54]. These findings are supported by the WKB shadow estimate obtained from the study of quasinormal modes in the eikonal limit.

The organization of this paper is as follows: In section II, we discuss the propagation of a massless scalar field in the background of a black hole on a thin brane-world known as the Randall-Sundrum model (RSII), described by a warped geometry theory. In Sec. III, we have determined the quasinormal modes for a scalar perturbation on this background wherein eventual effects of the fifth dimension must become relevant. Therefore, we use the WKB approximation, aiming to determine the quasinormal frequencies in the eikonal limit. In Sec. IV, we investigate the null geodesic curves to find the shadow radius of the RSII black hole, and we compare it with the prediction obtained from the eikonal quasinormal frequencies. In this case, we find deviations in the shadow radius of the black hole owing to the extra-dimensional curvature radius. From the EHT observational data, we present the imposed constraints on the AdS_5 curvature radius ℓ . The concluding remarks and the main results are given in Sec. V.

II. BLACK HOLES ON A THIN BRANE: THE RADIAL EQUATION

In this section, we aim to describe the dynamics of a massless scalar field propagating on a thin brane-world background. Thus, we start by considering the Garriga-Tanaka solution that, at the first-order approximation of GM , describes the metric of a matter distribution with mass M localized in the brane [52],

$$ds^2 = -f(r)dt^2 + \frac{dr^2}{g(r)} + r^2d\Omega^2, \quad (1)$$

where, in the weak field limit ($r \gg \ell$) from the horizon of matter after the collapse, we get

$$f(r) = 1 - \frac{2M}{r} - \frac{4M\ell^2}{3r^3}, \quad \text{and} \quad g(r) = 1 - \frac{2M}{r} - \frac{2M\ell^2}{3r^3}, \quad (2)$$

in which ℓ is the curvature radius of AdS_5 , and we consider unities $c = G = 1$. In this scenario, we may discuss the propagation of a massless scalar field and obtain the radial equation by using the Klein–Gordon equation

$$\frac{1}{\sqrt{-g}}\partial_\mu (\sqrt{-g}g^{\mu\nu}\partial_\nu\Psi) = 0. \quad (3)$$

For the sake of simplicity, one may use the following separation of variables

$$\Psi_{\omega lm}(\vec{r}, t) = \frac{\mathcal{R}_{\omega l}(r)}{r} Y_{lm}(\theta, \phi) e^{-i\omega t}, \quad (4)$$

where $Y_{lm}(\theta, \phi)$ are the spherical harmonics, ω is the frequency and l is the multipole number. Thus, substituting the expression (4) into equation (3), one finds the following radial equation for $\mathcal{R}_{\omega l}$

$$\Lambda(r)\frac{d}{dr}\left[\Lambda(r)\frac{d\mathcal{R}_{\omega l}}{dr}\right] + (\omega^2 - V_{eff})\mathcal{R}_{\omega l} = 0. \quad (5)$$

Here, the effective potential is given by

$$V_{eff} = \frac{\Lambda(r)}{r}\frac{d\Lambda(r)}{dr} + \frac{f(r)}{r^2}l(l+1), \quad (6)$$

where $\Lambda(r) = \sqrt{g(r)f(r)}$. In order to analyze the radial equation (5), by considering the asymptotic limits, we can introduce a new coordinate $dx = \Lambda(r)^{-1}dr$ (commonly called tortoise coordinate) so that equation (5) reduces to a Schrödinger-type equation, as follows

$$\frac{d^2\mathcal{R}_{\omega l}}{dx^2} + (\omega^2 - V_{eff})\mathcal{R}_{\omega l} = 0. \quad (7)$$

As we will see below, this analysis will allow us to estimate the shadow radius by calculating the quasinormal modes in the eikonal limit, which corresponds to the limit to a large multipole number l .

III. EIKONAL QUASINORMAL MODES IN THE WARPED BRANE-WORLD

Quasinormal modes are solutions of the perturbation equation (7) that satisfy specific boundary conditions. In this case, it is possible to consider two different solutions obtained to the radial equation written in terms of the new coordinate by assuming some set of boundary conditions [55]. Furthermore, these solutions present a discrete quasinormal frequency spectrum $\omega = \omega_R + i\omega_I$, where the real part (ω_R) determines the oscillation frequency, while

the imaginary part (ω_I) determines the decay rate. In a regime for which the real part of the QNM frequency is large, one has the called eikonal limit. On its turn, WKB approximation has been applied to obtain the quasinormal modes in black hole for decades [39–41]. This method is widely employed in the literature due to its practical means of finding approximating solutions compared to numerical methods, in addition to providing accurate predictive results [36, 37, 42]. The WKB method in the eikonal limit yields an accurate estimate for the quasinormal frequencies from the wave equation (7). Specifically, the QNM frequencies in this particular limit can be obtained from the following expression

$$\frac{i(\omega_n^2 - V_0)}{\sqrt{-2V_0''}} = n + \frac{1}{2}, \quad (8)$$

where n is the harmonic number, V_0 is the maximum effective potential evaluated at the point r_0 , the prime ($'$) denotes derivation with respect to the tortoise coordinate x . Furthermore, the effective potential (6) at the eikonal limit ($l \rightarrow \infty$) is $V_{eff} \approx f(r)l^2/r^2$, so that the equation (8) can be written in the form

$$\omega_n \approx \frac{l\sqrt{f(r_0)}}{r_0} - \frac{i(n + 1/2)}{\sqrt{2}} \sqrt{-\frac{r_0^2}{f(r_0)} \frac{d^2}{dx^2} \left[\frac{f(r)}{r^2} \right]_{r=r_0}}, \quad (9)$$

which corresponds to the quasinormal frequency to the overtone mode n . In Fig. 1, one can see that both parts, real and imaginary, of eikonal quasinormal frequencies remain finite. In principle, the value of the AdS_5 curvature radius ℓ must be constrained just from the empirical data such that the quasinormal frequencies will tend to zero in the eikonal limit for large values of the ℓ -parameter. Furthermore, the result (9) obtained by assuming the eikonal limit will be compared with the null geodesics parameters, as we will see in the next section. From computing the deviations on the black hole shadow radius in the brane-world model, we will impose bounds on the curvature radius AdS_5 .

IV. CORRECTED SHADOW RADIUS OF THE BRANE-WORLD BLACK HOLE

In this section, we will study the null geodesic, aiming to investigate the influence of the extra dimension on the critical impact and critical radius parameters. This approach will also allow us to determine the radius of the shadow of the Garriga-Tanaka (RSII) black hole.

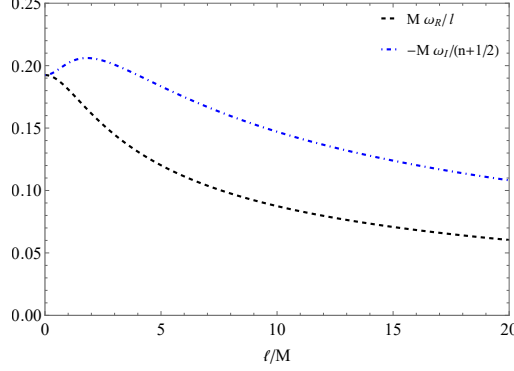


FIG. 1: Real and negative imaginary parts of the eikonal quasinormal frequencies as function of the AdS_5 curvature radius.

From this investigation, we will find bounds on the curvature radius of the AdS_5 spacetime. We begin by considering the following Lagrangian density

$$\mathcal{L} \equiv \frac{1}{2} g_{\mu\nu} \dot{x}^\mu \dot{x}^\nu, \quad (10)$$

where the dot denotes the derivative with respect to the affine parameter. Now, applying the line element (1), we have

$$2\mathcal{L} = f(r) \dot{t}^2 - \frac{\dot{r}^2}{g(r)} - r^2 \left(\dot{\theta}^2 + \sin^2 \theta \dot{\phi}^2 \right). \quad (11)$$

For the sake of simplicity, at this point, by setting the angle $\theta = \pi/2$, one can examine the motion in an equatorial plane. Thus, we can find the equation of motion for the Hamilton-Jacobi equation

$$E = f(r) \dot{t}, \quad L = r^2 \dot{\phi}, \quad (12)$$

where E and L are the constants corresponding to energy and angular momentum, respectively. For a null geodesic, we have $g_{\mu\nu} \dot{x}^\mu \dot{x}^\nu = 0$, and we can find the following expression

$$\dot{r}^2 + \mathcal{V}(r) = 0, \quad \mathcal{V}(r) = \frac{g(r)}{f(r)} E^2 - g(r) \frac{L^2}{r^2}. \quad (13)$$

Now, just for convenience, we can introduce a new variable $u = 1/r$ to write the orbital equation

$$\left(\frac{du}{d\phi} \right)^2 = \frac{(3 - 6Mu - 2M\ell^2u^3)}{(3 - 6Mu - 4M\ell^2u^3) b^2} - \left(1 - 2Mu - \frac{2M\ell^2u^3}{3} \right) u^2, \quad (14)$$

$$\frac{d^2u}{d\phi^2} = \frac{2M\ell^2 (3 - 4Mu) u^2}{b^2 (6Mu + 4M\ell^2u^3 - 3)^2} - \left(1 - 3Mu - \frac{5M\ell^2u^3}{3} \right) u. \quad (15)$$

Here, we have that $b = L/E$ is the impact parameter defined as the perpendicular distance (measured from infinity) between the geodesic and the parallel line that passes through the origin. Using the following critical conditions, (i) $\mathcal{V}(r_c) = 0$ and (ii) $d\mathcal{V}(r)/dr|_{r=r_c} = 0$, we can obtain the critical impact parameter from a system of equations with which one relates the impact parameter to the critical radius, as follows

$$b_c^2 = \frac{r_c^2}{f(r_c)} = \frac{3r_c^5}{3r_c^3 - 6Mr_c^2 - 4M\ell^2}. \quad (16)$$

Notice that r_c corresponds to the radius of photon circular orbit. On its turn, the critical conditions expressed by (ii) yield a polynomial equation that is used to determine the critical radius:

$$20\ell^4 M^2 + 6\ell^2 M (13M - 6r_c) r_c^2 + 9r_c^4 (6M^2 - 5Mr_c + r_c^2) = 0. \quad (17)$$

We must highlight that, here, we want to study the trajectory of a ray of light in the spherically symmetric Garriga-Tanaka background. Specifically, when we analyze the ray in a plane, we observe that any ray of light that starts at a particular angle θ must keep the same angle throughout its path. In Figure 2, we have found some results for the critical impact parameter from the numerical solution of the orbit equations (14) and (15). In this case, we have obtained the geodesic trajectory (blue thick curve) computed for the impact parameter $b = 5.5M$. Therefore, as a direct influence of the existence of the extra-dimensional parameter ℓ , we observed an increase in the absorption section. Furthermore, in Figure 2, whereas the black disk depicts the limit of the event horizon, the critical radius for the photon sphere is shown as an internal dotted circle. In turn, the critical impact parameter (black hole shadow) is shown by an external dashed circle.

Finally, one can estimate the size of the radius of the black hole shadow by using the study of geodesic curves that we might express via celestial coordinates [56]

$$\alpha = \lim_{r_o \rightarrow \infty} \left[-r_o^2 \sin \theta_o \frac{d\phi}{dr} \Big|_{\theta=\theta_o} \right], \quad (18)$$

$$\beta = \lim_{r_o \rightarrow \infty} \left[r_o^2 \frac{d\theta}{dr} \Big|_{\theta=\theta_o} \right], \quad (19)$$

where (r_o, θ_o) is the position of the observer at infinity. Thus, for an observer on an equatorial plane $\theta_o = \pi/2$, we have the following relationship for the shadow radius

$$R_s \equiv \sqrt{\alpha^2 + \beta^2} = \sqrt{\frac{3r_c^5}{3r_c^3 - 6Mr_c^2 - 4M\ell^2}}. \quad (20)$$

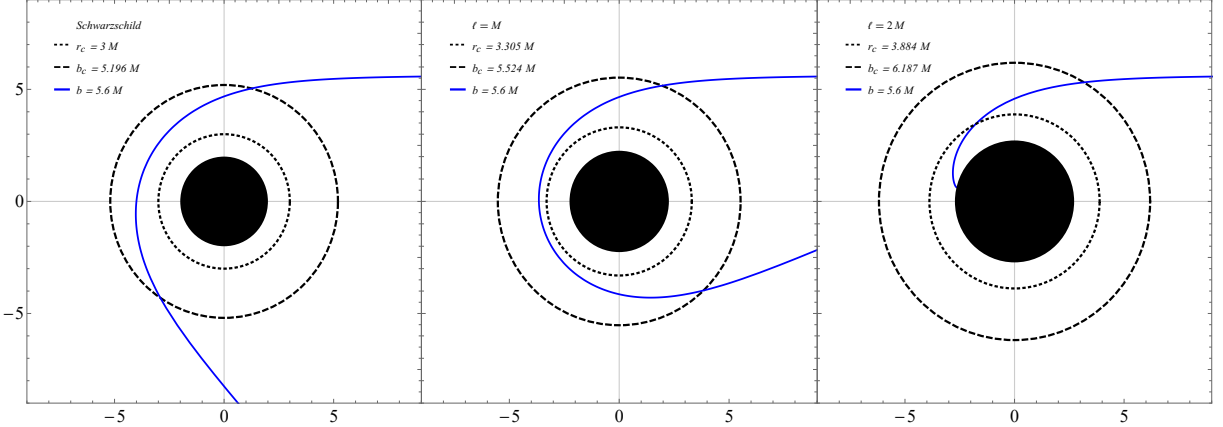


FIG. 2: Null geodesic in polar coordinates for different values of ℓ , in which we consider a test beam of light by keeping the impact parameter, $b = 5.6M$, fixed.

Let us now expand the radius of the shadow up to order (ℓ^2/M^2) by assuming that the contribution arising from extra-dimension is a small correction to R_s , $\ell/M \ll 1$, so that

$$R_s \approx 3\sqrt{3}M \left[1 + \frac{2}{27} \frac{\ell^2}{M^2} + \mathcal{O}\left(\frac{\ell^4}{M^4}\right) \right]. \quad (21)$$

On the other hand, for a spherically symmetric and asymptotically flat static geometry, Cardoso *et al.* [57] showed that, in the eikonal limit, the quasinormal modes are determined by the parameters of the null circular geodesic so that $\Omega_c = \dot{\phi}/\dot{t}$ is the angular velocity for the last null circular orbit, and $\lambda = \sqrt{\mathcal{V}''(r)/2\dot{t}^2}$ is the Lyapunov exponent that determines the unstable time scale of the orbit. By directly comparing with equation (9), we can write the equation for quasinormal frequencies in the form

$$\omega_n = \Omega_c l - i(n + 1/2)|\lambda|. \quad (22)$$

It is worth to mention that there are violations in this relationship, as shown by Konoplya and Stuchlík [58] when considering a black hole in the Einstein-Lovelock theory. Since we know the form of the angular velocity Ω_c , one can use equations (12) and (16) to obtain its relationship with the critical impact parameter $\Omega_c = (f(r_c)b_c)/r_c^2 = 1/b_c$. This equation highlights the correspondence relationship between the maximum value point of the effective potential (r_0) and the radius of the photon circular orbit (r_c) [see equations (9) and (22)]. Finally, in the eikonal regime $l \gg 1$, we have the relationship between the real part of the

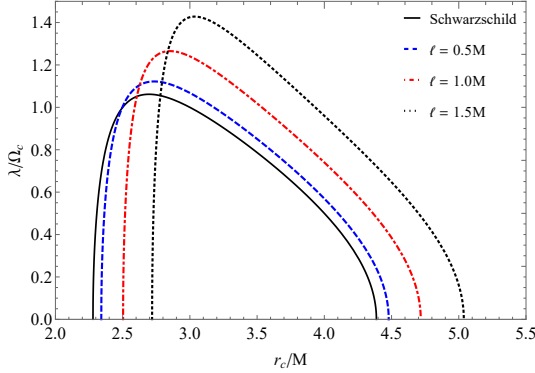


FIG. 3: Lyapunov exponent normalized by the angular velocity (λ/Ω_c), as function of r_c/M for some values of ℓ .

quasinormal modes and the shadow radius,

$$Re(\omega) = \lim_{l \gg 1} \left(\frac{l}{R_s} \right). \quad (23)$$

Notice that the estimate (23) may be employed to confirm the prediction (21). Hence, we can use it to compare with experimental data in order to constrain the found deviations. Besides, equation (22) shows that the real and imaginary parts of the quasinormal modes in the eikonal limit are related to the orbital angular velocity and the instability time scale of circular null geodesics, respectively. The instability of null circular orbits can be determined by the instability exponent, which is defined by the ratio of the Lyapunov exponent to the angular frequency. In Fig.3, we see the variation of the instability exponent in relation to the radius r_c . The maximum of the instability increases with the increase in the contribution coming from the extra dimension. On the other hand, the instability decreases as r_c increases.

A. Constraints on the AdS_5 curvature radius

As we saw above, we obtained deviations in the black hole shadow radius owing to the existence of an extra dimension. On its turn, if we turn off the extra-dimensional effects ($\ell = 0$), we recover the well-known results for the Schwarzschild background. Although this independent approach allows us to search for traces of extra dimensions, imposing constraints on deviations found, once the curvature radius ℓ is positively correlated to the shadow radius, and given the low-precision measurements, thus we must have a weakening

in the predicted bounds compared to sub-mm gravity experiments, for instance.

In our analysis, we will follow the methodology developed in [59], aiming to obtain bounds on the AdS_5 curvature radius. Therefore, the observed angular radius – which has ring-like features in the horizon-scale EHT image of Sgr A* –, must be compared to the theoretically determined angular radius of the black hole shadow. From the precise determination of both mass and distance of Sgr A*, the central supermassive black hole of our galaxy, we can verify the accordance, within the uncertainty allowed, between the predicted theoretical results by this study and the empirical data found by the EHT observations [60]. On its turn, the mass and distance of Sgr A* have been studied over the last few decades by exploring the dynamics of star clusters and, in particular, the movement of stars close to the center of the galaxy. According to Ref. [59], the shadow radius measurements are restricted to the following regions determined by the average between the estimates based on the VLTI and Keck instruments, within 1σ and 2σ intervals, respectively,

$$4.55 \lesssim R_s/M \lesssim 5.22, \quad \text{and} \quad 4.21 \lesssim R_s/M \lesssim 5.56. \quad (24)$$

In Figure 4a, we show the expected deviations in the behavior of the shadow radius owing to the extra dimension. As we see, the increase in the AdS_5 curvature radius ℓ results in a consequent increase in the radius of the black hole shadow. In our analysis, we have considered the average in the mass from KECK- and VLTI-based estimates. Therefore, from the empirical data obtained by observations of EHT, we can impose the limits on curvature radius at the 95% confidence level (CL), such that $\ell \lesssim 6.5 \times 10^9 \text{ m} \simeq 4.3 \times 10^{-2} \text{ AU}$, as shown in Figure 4b. At this point, we can compare our results with another which investigates similar physical systems. In this case, the absence of deviations on observation of the highly circular shadow of black hole M87* provides constraints on the AdS_5 radius so that $\ell \lesssim 170 \text{ AU}$ [28]. In turn, the first bounds obtained on the extra dimensions by the study of the time-lag between the detection of gravitational waves (GW) and electromagnetic (EM) signals from the merging of a binary system detected by the event GW170817 have established at 68% CL an upper limit of $\ell \lesssim 0.535 \text{ Mpc} \simeq 1.10 \times 10^{11} \text{ AU}$ [29], whereas our analysis found $\ell \lesssim 1.0 \times 10^{-2} \text{ AU}$ for the same confidence interval. It is worth mentioning that, as we have seen, our study yields stronger constraints than those found by similar physical systems, according to the best of our knowledge. Ultimately, although we obtained weaker constraints compared to results obtained from sub-mm scale gravity experiments,

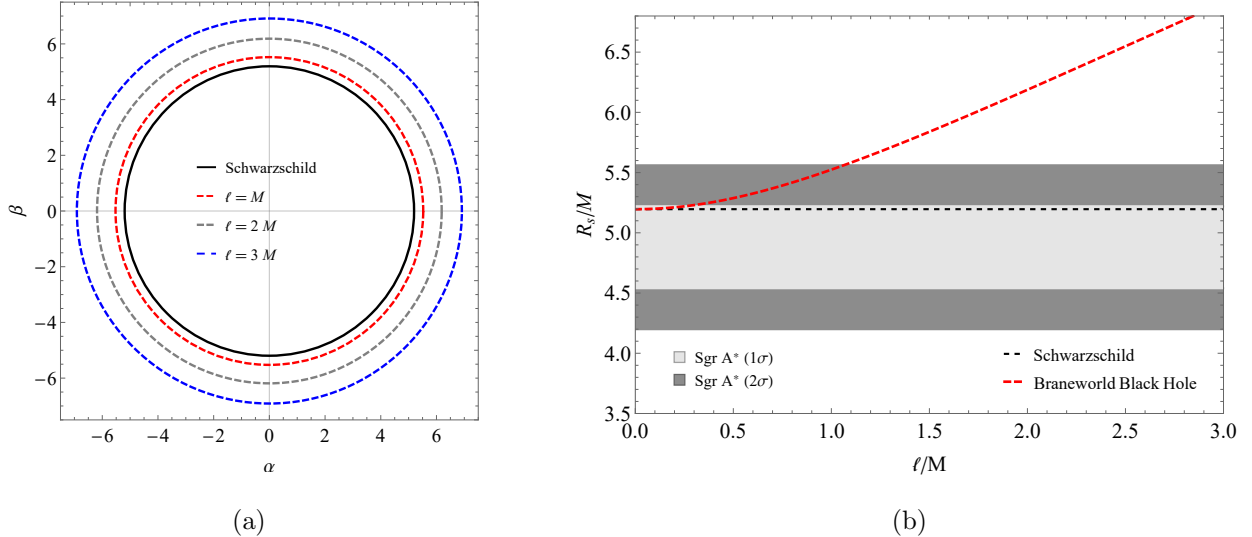


FIG. 4: The left panel shows the changes in the behavior of the shadow radius with the variation of the AdS_5 radius ℓ . In turn, in the right panel, we found bounds from the direct comparison between the results obtained by our theoretical analysis with the EHT experimental data.

this approach has set independent limits and can aid the investigation of the geometric structure of the universe.

V. FINAL REMARKS

Recently, higher-dimensional theories have drawn increasing attention. As has been pointed out, the seek for evidence of large extra dimensions has been performed in several experimental researches, making its detection a challenging problem in itself. In this work, we have studied the quasinormal modes of a black hole in a brane-world model, aiming to search for traces of extra dimensions. By employing the WKB method, we compute the eikonal quasinormal frequencies. This complementary analysis also allowed us to confirm the theoretical prediction for the black hole shadow radius from the convergence between the WKB- and null geodesics-method estimates.

From recent measurements of the shadow image of Sgr A* – a supermassive black hole in the center of our galaxy – we estimate deviations owing to an extra dimension in the RSII scenario on the theoretical shadow radius predicted. Given the inaccuracy involving the measured spin of Sgr A*, which may even be zero but still can provide compatible results

with recent measures [54], we explore the possibility of describing them as a non-rotating RSII black hole. In this case, we have considered the Garriga-Tanaka solution that takes a classical approach to linearized brane-world gravity and describes a black hole solution in the weak field limit.

As we saw, the curvature radius of the AdS_5 spacetime is positively correlated to the shadow radius so that the increasing/decreasing in one leads to correspondingly increasing/decreasing in the other. Furthermore, we found that $\ell = 0$, i.e., in the absence of new physics coming from extra dimension, one recovers the standard estimates expected for the Schwarzschild background. By investigating the null geodesic curves, we determine the shadow of the RSII black hole. From recent observational data of the shadow of Sgr A* released by the Event Horizon Telescope collaboration, one may impose constraints on the curvature radius of AdS_5 spacetime. Therefore, we find more stringent limits on $\ell \lesssim 4.3 \times 10^{-2}$ AU (at 95% CL) than previously obtained for similar physical systems, to the best of our knowledge. Moreover, non-zero predicted curvature radius also leads to agreement with the observed shadow radius within 68% confidence interval, providing $\ell \lesssim 1.0 \times 10^{-2}$ AU.

We would like to highlight that although our analysis provides weaker bounds than those obtained from collider experiments or sub-mm precision gravity tests, which have set limits on the non-Newtonian force, in this study, we have provided conservative bounds since limits ourselves to investigate the shadow radius in a non-rotating RSII-type black hole background. Further, the bounds reported by us have been obtained in a manner complementary to the studies previously mentioned. Finally, the newly begun era of observational astronomy opens several avenues for future research that might be explored to obtain new constraints on the AdS_5 curvature radius, for instance, or even to test extensions of general relativity, therefore shedding light into seeking for physics beyond the SM.

Acknowledgments

We would like to thank CNPq, CAPES and CNPq/PRONEX/FAPESQ-PB (Grant No. 165/2018), for partial financial support. FAB acknowledges support from CNPq (Grant No. 309092/2022–1). ASL acknowledges support from CAPES (Grant No. 88887.800922/2023–00). JAVC would like to thank FAPESQ-PB/CNPq (Grant No. 077/2022) for financial

support.

- [1] G. Nordstrom, “On the possibility of unifying the electromagnetic and the gravitational fields,” *Phys. Z.*, vol. 15, pp. 504–506, 1914.
- [2] T. Kaluza, “Zum Unitätsproblem der Physik,” *Sitzungsber. Preuss. Akad. Wiss. Berlin (Math. Phys.)*, vol. 1921, pp. 966–972, 1921.
- [3] O. Klein, “Quantum Theory and Five-Dimensional Theory of Relativity. (In German and English),” *Z. Phys.*, vol. 37, pp. 895–906, 1926.
- [4] I. Antoniadis, N. Arkani-Hamed, S. Dimopoulos, and G. R. Dvali, “New dimensions at a millimeter to a Fermi and superstrings at a TeV,” *Phys. Lett. B*, vol. 436, pp. 257–263, 1998.
- [5] N. Arkani-Hamed, S. Dimopoulos, and G. R. Dvali, “The Hierarchy problem and new dimensions at a millimeter,” *Phys. Lett. B*, vol. 429, pp. 263–272, 1998.
- [6] N. Arkani-Hamed, S. Dimopoulos, and G. R. Dvali, “Phenomenology, astrophysics and cosmology of theories with submillimeter dimensions and TeV scale quantum gravity,” *Phys. Rev. D*, vol. 59, p. 086004, 1999.
- [7] L. Randall and R. Sundrum, “A Large mass hierarchy from a small extra dimension,” *Phys. Rev. Lett.*, vol. 83, pp. 3370–3373, 1999.
- [8] L. Randall and R. Sundrum, “An Alternative to compactification,” *Phys. Rev. Lett.*, vol. 83, pp. 4690–4693, 1999.
- [9] R. L. Workman *et al.*, “Review of Particle Physics,” *PTEP*, vol. 2022, p. 083C01, 2022.
- [10] G. Aad *et al.*, “Search for new phenomena in events with an energetic jet and missing transverse momentum in pp collisions at $\sqrt{s} = 13$ TeV with the ATLAS detector,” *Phys. Rev. D*, vol. 103, no. 11, p. 112006, 2021.
- [11] S. Hannestad and G. G. Raffelt, “Supernova and neutron star limits on large extra dimensions reexamined,” *Phys. Rev. D*, vol. 67, p. 125008, 2003. [Erratum: *Phys. Rev. D* 69, 029901 (2004)].
- [12] E. G. Adelberger, J. H. Gundlach, B. R. Heckel, S. Hoedl, and S. Schlamminger, “Torsion balance experiments: A low-energy frontier of particle physics,” *Prog. Part. Nucl. Phys.*, vol. 62, pp. 102–134, 2009.
- [13] J. Murata and S. Tanaka, “A review of short-range gravity experiments in the LHC era,” *Class. Quant. Grav.*, vol. 32, no. 3, p. 033001, 2015.

[14] F. Dahia and A. S. Lemos, “Constraints on extra dimensions from atomic spectroscopy,” *Phys. Rev. D*, vol. 94, no. 8, p. 084033, 2016.

[15] F. Dahia and A. S. Lemos, “Is the proton radius puzzle evidence of extra dimensions?,” *Eur. Phys. J. C*, vol. 76, no. 8, p. 435, 2016.

[16] F. Dahia, E. Maciel, and A. S. Lemos, “Rydberg states of hydrogenlike ions in a braneworld model,” *Eur. Phys. J. C*, vol. 78, no. 6, p. 526, 2018.

[17] A. S. Lemos, G. C. Luna, E. Maciel, and F. Dahia, “Spectroscopic tests for short-range modifications of Newtonian and post-Newtonian potentials,” *Class. Quant. Grav.*, vol. 36, no. 24, p. 245021, 2019.

[18] A. S. Lemos, “Submillimeter constraints for non-Newtonian gravity from spectroscopy,” *EPL*, vol. 135, no. 1, p. 11001, 2021.

[19] F. Luo and H. Liu, “Exploring extra dimensions in spectroscopy experiments,” *Chin. Phys. Lett.*, vol. 23, p. 2903, 2006.

[20] L. Zhi-gang, W.-T. Ni, and A. P. Paton, “Extra dimensions and atomic transition frequencies,” *Chin. Phys. B*, vol. 17, pp. 70–76, 2008.

[21] E. J. Salumbides, A. N. Schellekens, B. Gato-Rivera, and W. Ubachs, “Constraints on extra dimensions from precision molecular spectroscopy,” *New J. Phys.*, vol. 17, no. 3, p. 033015, 2015.

[22] A. M. Sirunyan *et al.*, “Search for black holes and sphalerons in high-multiplicity final states in proton-proton collisions at $\sqrt{s} = 13$ TeV,” *JHEP*, vol. 11, p. 042, 2018.

[23] G. Aad *et al.*, “Search for strong gravity in multijet final states produced in pp collisions at $\sqrt{s} = 13$ TeV using the ATLAS detector at the LHC,” *JHEP*, vol. 03, p. 026, 2016.

[24] R. Emparan, J. Garcia-Bellido, and N. Kaloper, “Black hole astrophysics in AdS brane worlds,” *JHEP*, vol. 01, p. 079, 2003.

[25] S. S. Bohra, S. Sarkar, and A. A. Sen, “Gravitational atoms in the braneworld scenario,” *Phys. Rev. D*, vol. 109, p. 104021, 2024.

[26] A. Chrysostomou, A. Cornell, A. Deandrea, E. Ligout, and D. Tsimpis, “Black holes and nilmanifolds: quasinormal modes as the fingerprints of extra dimensions?,” *Eur. Phys. J. C*, vol. 83, no. 4, p. 325, 2023.

[27] S. T. McWilliams, “Constraining the braneworld with gravitational wave observations,” *Phys. Rev. Lett.*, vol. 104, p. 141601, 2010.

[28] S. Vagnozzi and L. Visinelli, “Hunting for extra dimensions in the shadow of M87*,” *Phys. Rev. D*, vol. 100, no. 2, p. 024020, 2019.

[29] L. Visinelli, N. Bolis, and S. Vagnozzi, “Brane-world extra dimensions in light of GW170817,” *Phys. Rev. D*, vol. 97, no. 6, p. 064039, 2018.

[30] A. K. Mishra, A. Ghosh, and S. Chakraborty, “Constraining extra dimensions using observations of black hole quasi-normal modes,” *Eur. Phys. J. C*, vol. 82, no. 9, p. 820, 2022.

[31] B. P. Abbott *et al.*, “Observation of Gravitational Waves from a Binary Black Hole Merger,” *Phys. Rev. Lett.*, vol. 116, no. 6, p. 061102, 2016.

[32] B. P. Abbott *et al.*, “GW170817: Observation of Gravitational Waves from a Binary Neutron Star Inspiral,” *Phys. Rev. Lett.*, vol. 119, no. 16, p. 161101, 2017.

[33] V. Cardoso, R. Konoplya, and J. P. Lemos, “Quasinormal frequencies of schwarzschild black holes in anti-de sitter spacetimes: a complete study of the overtone asymptotic behavior,” *Physical Review D*, vol. 68, no. 4, p. 044024, 2003.

[34] V. Cardoso, M. Kimura, A. Maselli, E. Berti, C. F. Macedo, and R. McManus, “Parametrized black hole quasinormal ringdown: Decoupled equations for nonrotating black holes,” *Physical Review D*, vol. 99, no. 10, p. 104077, 2019.

[35] M. Cruz, F. Brito, and C. Silva, “Polar gravitational perturbations and quasinormal modes of a loop quantum gravity black hole,” *Physical Review D*, vol. 102, no. 4, p. 044063, 2020.

[36] M. A. Anacleto, J. Campos, F. A. Brito, and E. Passos, “Quasinormal modes and shadow of a schwarzschild black hole with gup,” *Annals of Physics*, vol. 434, p. 168662, 2021.

[37] J. Campos, M. Anacleto, F. Brito, and E. Passos, “Quasinormal modes and shadow of non-commutative black hole,” *Scientific Reports*, vol. 12, no. 1, p. 8516, 2022.

[38] R. Konoplya and A. Zhidenko, “Quasinormal modes of black holes: From astrophysics to string theory,” *Reviews of Modern Physics*, vol. 83, no. 3, p. 793, 2011.

[39] B. F. Schutz and C. M. Will, “Black hole normal modes: a semianalytic approach,” *The Astrophysical Journal*, vol. 291, pp. L33–L36, 1985.

[40] S. Iyer and C. M. Will, “Black-hole normal modes: A wkb approach. i. foundations and application of a higher-order wkb analysis of potential-barrier scattering,” *Physical Review D*, vol. 35, no. 12, p. 3621, 1987.

[41] R. Konoplya, “Quasinormal behavior of the d-dimensional schwarzschild black hole and the higher order wkb approach,” *Physical Review D*, vol. 68, no. 2, p. 024018, 2003.

[42] R. Konoplya, A. Zhidenko, and A. Zinhailo, “Higher order wkb formula for quasinormal modes and grey-body factors: recipes for quick and accurate calculations,” *Classical and Quantum Gravity*, vol. 36, no. 15, p. 155002, 2019.

[43] S. Chakraborty, K. Chakravarti, S. Bose, and S. SenGupta, “Signatures of extra dimensions in gravitational waves from black hole quasinormal modes,” *Phys. Rev. D*, vol. 97, no. 10, p. 104053, 2018.

[44] R. Dey, S. Biswas, and S. Chakraborty, “Ergoregion instability and echoes for braneworld black holes: Scalar, electromagnetic, and gravitational perturbations,” *Phys. Rev. D*, vol. 103, no. 8, p. 084019, 2021.

[45] S. S. Hashemi, M. Kord Zangeneh, and M. Faizal, “Charged scalar quasi-normal modes for higher-dimensional Born–Infeld dilatonic black holes with Lifshitz scaling,” *Eur. Phys. J. C*, vol. 80, no. 2, p. 111, 2020.

[46] V. Cardoso, J. P. S. Lemos, and S. Yoshida, “Quasinormal modes of Schwarzschild black holes in four-dimensions and higher dimensions,” *Phys. Rev. D*, vol. 69, p. 044004, 2004.

[47] M. A. Anacleto, J. A. V. Campos, F. A. Brito, E. Maciel, and E. Passos, “Scattering and absorption by extra-dimensional black holes with GUP,” [arXiv:2307.09536 [gr-qc]].

[48] K. Akiyama *et al.*, “First M87 Event Horizon Telescope Results. I. The Shadow of the Supermassive Black Hole,” *Astrophys. J. Lett.*, vol. 875, p. L1, 2019.

[49] K. Akiyama *et al.*, “First M87 Event Horizon Telescope Results. VI. The Shadow and Mass of the Central Black Hole,” *Astrophys. J. Lett.*, vol. 875, no. 1, p. L6, 2019.

[50] K. Akiyama *et al.*, “First Sagittarius A* Event Horizon Telescope Results. VI. Testing the Black Hole Metric,” *Astrophys. J. Lett.*, vol. 930, no. 2, p. L17, 2022.

[51] K. Akiyama *et al.*, “First Sagittarius A* Event Horizon Telescope Results. I. The Shadow of the Supermassive Black Hole in the Center of the Milky Way,” *Astrophys. J. Lett.*, vol. 930, no. 2, p. L12, 2022.

[52] J. Garriga and T. Tanaka, “Gravity in the brane world,” *Phys. Rev. Lett.*, vol. 84, pp. 2778–2781, 2000.

[53] I. Banerjee, S. Chakraborty, and S. SenGupta, “Hunting extra dimensions in the shadow of Sgr A*,” *Phys. Rev. D*, vol. 106, no. 8, p. 084051, 2022.

[54] G. Fragione and A. Loeb, “An upper limit on the spin of SgrA* based on stellar orbits in its vicinity,” *Astrophys. J. Lett.*, vol. 901, no. 2, p. L32, 2020.

- [55] E. Berti, V. Cardoso, and A. O. Starinets, “Quasinormal modes of black holes and black branes,” *Classical and Quantum Gravity*, vol. 26, no. 16, p. 163001, 2009.
- [56] S. E. Vazquez and E. P. Esteban, “Strong field gravitational lensing by a Kerr black hole,” *Nuovo Cim. B*, vol. 119, pp. 489–519, 2004.
- [57] V. Cardoso, A. S. Miranda, E. Berti, H. Witek, and V. T. Zanchin, “Geodesic stability, lyapunov exponents, and quasinormal modes,” *Physical Review D*, vol. 79, no. 6, p. 064016, 2009.
- [58] R. Konoplya and Z. Stuchlk, “Are eikonal quasinormal modes linked to the unstable circular null geodesics?,” *Physics Letters B*, vol. 771, pp. 597–602, 2017.
- [59] S. Vagnozzi, R. Roy, Y.-D. Tsai, L. Visinelli, M. Afrin, A. Allahyari, P. Bambhaniya, D. Dey, S. G. Ghosh, P. S. Joshi, *et al.*, “Horizon-scale tests of gravity theories and fundamental physics from the Event Horizon Telescope image of Sagittarius A,” *Class. Quant. Grav.*, vol. 40, no. 16, p. 165007, 2023.
- [60] K. Akiyama, J. Kauffmann, L. D. Matthews, K. Moriyama, S. Koyama, and K. Hada, “Millimeter/submillimeter vlbi with a next generation large radio telescope in the atacama desert,” *Galaxies*, vol. 11, no. 1, p. 1, 2022.